Acta Cryst. (1954). 7, 412

X-ray Diffraction by a Layer Structure Containing Random Displacements

BY W. COCHRAN AND E. R. HOWELLS†

Cavendish Laboratory, Cambridge, England

(*Received* 11 *February* 1954)

The diffraction pattern to be expected from crystals of imidazole methaemoglobin, which have an unusual type of fault structure, is calculated and found to agree well with the experimental observations.

The physical background of this problem has been explained in the preceding paper by Bragg & Howells (1954). Adopting the notation used by these authors, we label successive layers of molecules with the letters R and L. We begin by calculating the intensity distribution that would be given by the R-molecules only; the contribution of the L-molecules will be included later. At present no account will be taken of the repeat of the pattern in the a direction; this, too, will be allowed for later. Meantime we consider only the relative positions of a succession of representative R-molecules, one in each R-layer. Take a particular molecule as origin. The possible positions of molecules at horizontal distances of c, $2c$, $3c$ respectively are shown in Fig. 1. The numbers represent the probabilities of the positions being occupied, on the assumption that the first L-molecule (not shown) is as likely to be displaced by $\frac{1}{2}\varepsilon_0 a$ as by $-\frac{1}{2}\varepsilon_0 a$. Let us take c and $\varepsilon_0 a$ as units of distance horizontally and vertically, and denote the probability associated with the point (n, m) by $p(n, m)$. By analogy with the 'random-walk' problem, this is the Bernoullian distribution

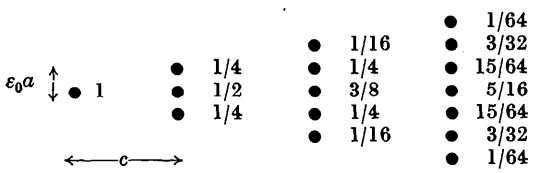

Fig. 1. The possible positions, with their probabilities, for a a few R-molecules.

$$p(n, m) = \frac{(2n)!}{(n+m)!\,(n-m)!}\,(\tfrac{1}{2})^{2n}\,. \qquad (1)$$

Suppose now that there is an infinite string of R-molecules in the c direction. Let us represent each molecule by a point at its centre, and then form the vector set (Patterson function) of this set of points. It will be a non-periodic distribution of points *whose relative weights are just the values of* $p(n, m)$. It will also be centrosymmetrical, and Fig. 1 therefore gives a small section of this Patterson function on the right of the origin. Thus $p(-n, m) = p(n, m)$.

We now make use of the fact that the Fourier transform of the Patterson function gives the distribution of *intensity* in reciprocal space. Taking coordinates (ξ, ζ) in reciprocal space such that $\xi = 1$ corresponds to a distance c^* from the origin while $\zeta = 1$ corresponds to a perpendicular distance $(\varepsilon_0 a)^*$, the required transform is

$$S_1(\xi, \zeta) = \sum_{n=-\infty}^{+\infty} \sum_{m=-n}^{+n} p(n, m) \cos 2\pi m\zeta \cos 2\pi n\xi\,. \quad (2)$$

This is the intensity that corresponds to each of the infinite chain of R-molecules being represented by a point. Replacing points by molecules of structure factor $F_R(\xi, \zeta)$, the actual intensity becomes $S_1(\xi, \zeta)F_R^2(\xi, \zeta)$.

To evaluate S_1, we consider first the summation over m. It is found that

$$\sum_{m=-n}^{+n} \frac{(2n)!}{(n+m)!\,(n-m)!}\,(\tfrac{1}{2})^{2n} \cos 2\pi m\zeta = (\cos \pi\zeta)^{2n}\,. \quad (3)$$

(This result may be verified by expanding the right-hand side, in the form $\{\frac{1}{2}(\exp[\pi i\zeta]+\exp[-\pi i\zeta])\}^{2n}$, by the binomial expansion, and comparing individual terms with those on the left hand side.) The next step is the evaluation of

$$S_1(\xi, \zeta) = 2\sum_{n=0}^{+\infty} (\cos \pi\zeta)^{2n} \cos 2\pi n\xi\,. \qquad (4)$$

We make use of the result

$$\sum_{n=0}^{\infty} x^n \cos n\alpha = \frac{1-x\cos\alpha}{1-2x\cos\alpha+x^2}\,,\ |x| < 1\,. \qquad (5)$$

Remembering that the term in (4) which has $n = 0$ must be given half the weight of any other, we find

$$S_1(\xi, \zeta) = \frac{1-\cos^4 \pi\zeta}{1-2\cos^2 \pi\zeta \cos 2\pi\xi+\cos^4 \pi\zeta}\,. \qquad (6)$$

We next consider how the contribution of the L-molecules to the intensity is to be allowed for. Taking the same origin as for Fig. 1, the possible positions and their probabilities for the first few of a string of L-molecules are shown in Fig. 2. Let $q(n, m)$ denote

† Now at Imperial Chemical Industries Ltd, Black Fan Road, Welwyn Garden City, Herts., England.

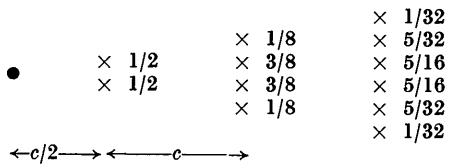

Fig. 2. Possible positions and probabilities for a few L-molecules. The origin is the same as for Fig. 1.

the probability associated with the point (n, m); n and m now assume half-integer values only. By comparison with Fig. 1 we see that

$$q(n, m) = \tfrac{1}{2}p(n-\tfrac{1}{2}, m-\tfrac{1}{2})+\tfrac{1}{2}p(n-\tfrac{1}{2}, m+\tfrac{1}{2}) \quad \text{for} \quad n \geqslant \tfrac{1}{2}. \quad (7)$$

By symmetry, $q(-n, m) = q(n, m)$.

The vectors between centres of molecules of type L coincide with those we have already considered, and we need only note that their contribution to the intensity will be

$$S_1(\xi, \zeta)F_L^2(\xi, \zeta).$$

Vectors between R and L molecules occur at points and with weights as shown (partly) in Fig. 2. By an argument similar to that already used, they contribute to the intensity an amount

$$S_2(\xi, \zeta).2F_R(\xi, \zeta)F_L(\xi, \zeta),$$

where

$$S_2(\xi, \zeta) = \sum_{n=-\infty}^{+\infty} \sum_{m=-n}^{+n} q(n, m) \cos 2\pi m\zeta \cos 2\pi n\xi. \quad (8)$$

It is understood that $n = \ldots -\frac{5}{2}, -\frac{3}{2}, -\frac{1}{2}, +\frac{1}{2} \ldots$.

Using the result (7), we find, as in deriving (3), that

$$\sum_{m=-n}^{+n} q(n, m) \cos 2\pi m\zeta = (\cos \pi\zeta)^{2n+1}. \quad (9)$$

Therefore

$$S_2(\xi, \zeta) = 2\sum_{n=\frac{1}{2}}^{\infty} (\cos \pi\zeta)^{2n+1} \cos 2\pi n\xi = \frac{2 \cos \pi\zeta(1-\cos^2 \pi\zeta) \cos \pi\xi}{1-2 \cos^2 \pi\zeta \cos 2\pi\xi+\cos^4 \pi\zeta}. \quad (10)$$

The derivation of (10) is similar to that of (6).

The complete expression for the intensity is now

$$I(\xi, \zeta) = S_1(\xi, \zeta)[F_R^2+F_L^2]+S_2(\xi, \zeta)[2F_RF_L]. \quad (11)$$

The final step is the introduction of the periodicity in the a direction. This will cause the continuous transform to be observable only along certain lines of constant ζ. Since we have chosen a scale such that $\zeta = 1$ corresponds to a distance $(\varepsilon_0 a)^{-1}$, the hth layer line from a crystal of spacing a will fall at $\zeta = (h/a)\varepsilon_0 a = h\varepsilon_0$.

Graphs of the functions S_1 and S_2 for various fixed values of ζ between 0·0 and 0·5 are shown in Fig. 3. The functions can be continued beyond the range shown by making use of their symmetry. S_1 has lines of symmetry at $\xi = 0, \frac{1}{2}$; $\zeta = 0, \frac{1}{2}$, while S_2 has lines of symmetry at $\xi = 0, \zeta = 0$ and lines of anti-symmetry at $\xi = \frac{1}{2}, \zeta = \frac{1}{2}$.

The results which we have obtained by using the 'Patterson function' concept can also be obtained by the method of Wilson (1949). Our approach is another way of attacking statistical mistake problems of general type.

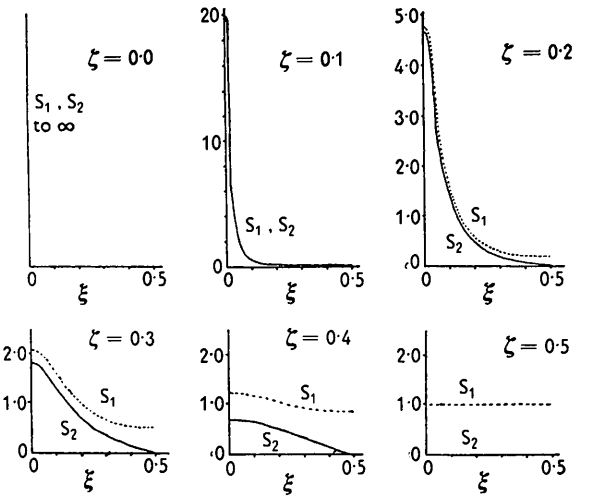

Fig. 3. Graphs of the functions $S_1(\xi, \zeta)$ and $S_2(\xi, \zeta)$ for various fixed values of ζ.

Comparison of results with those of Bragg & Howells

1. Inspection of (11) shows that the symmetry of the intensity distribution in the $(h0l)$ zone is mm. The crystal therefore diffracts X-rays as if it were orthorhombic.

2. It will be noticed from Fig. 3 that for $-0{\cdot}3<\zeta<0{\cdot}3$ we have $S_1 \approx S_2$. Equation (11) then reduces to

$$I(\xi, \zeta) = S_1(\xi, \zeta)[F_R \pm F_L]^2, \quad (12)$$

the positive sign applying when ξ is closest to an even integer, and vice versa. Again, in the range $0{\cdot}7<\zeta<1{\cdot}3$, we have $S_1 \approx -S_2$, so that (12) still holds, but the rule for choosing the sign is reversed.

3. When ζ is close to 0·5, 1·5 etc., $S_1 = 1$ and $S_2 = 0$ so that

$$I(\xi, \zeta) = F_R^2+F_L^2. \quad (13)$$

4. When $\zeta = 0$ the peaks of S_1 and of S_2 are infinitely narrow. For even orders $S_1 = S_2$, and for odd, $S_1 = -S_2$. Therefore, since $F_R = F_L$ in this case, only even orders are present on the zero layer.

5. For small values of ξ and of ζ the exact formulae (6) and (10) reduce to

$$S_1 = S_2 = \frac{2\zeta^2}{\pi^2\zeta^4+4\xi^2}. \quad (14)$$

In this range of ζ the variation of F_R and of F_L is much slower than that of S_1, and the latter will be

the only factor which governs the width of a peak. From (14) we find that in this range of ζ, each peak has an integral width of

$$\beta = \frac{\text{area}}{\text{maximum height}} = \tfrac{1}{2}\pi^2\zeta^2 .$$

For values of ζ close to 0·5, on the other hand, the molecular transform is the only factor governing the width of a peak, as shown by (13).

These five conclusions agree completely with those reached by Bragg & Howells (1954) on a more physical basis. We may note that their approximate calculation gave the 'total width' of a peak as $4\zeta^2$, whereas the exact formula gives the integral width as $\frac{1}{2}\pi^2\zeta^2$, for small values of ζ.

Comparison with experiment

Before comparing these results with experiment, allowance must be made for the fact that even the sharpest reflexions on the X-ray photograph have a finite 'instrumental width'. It will be remembered that the peaks of the intensity function are infinitely narrow when $\zeta = 0$. The corresponding reflexions have a breadth on the photograph which is just one half of the distance between successive reflexions. The density of a zero-layer spot is approximately constant across its breadth, and its integral width is therefore $\frac{1}{2}$, in units of c^*. For reflexions on layer lines which correspond to near-integer values of ζ, it has already been pointed out that the factor $S_1(\xi, \zeta)$ governs the width of the peak in reciprocal space. For other values of ζ, the reflexions on a particular layer line will not all have the same integral breadth. We can, however, find the breadth of an 'average' reflexion by taking F_R to be constant, and F_L to be zero. The integral width can then be shown to be given by

$$\beta = \tfrac{1}{2}\left[\int_{-\frac{1}{2}}^{+\frac{1}{2}} S_1(\xi, \zeta)\,d\xi\right]^{-1} .$$

Now

$$\int_a^b S_1(\xi, \zeta)\,d\xi = \left[\frac{\alpha}{\pi}\right]_a^b ,$$

where

$$\tan\alpha = \frac{1+\cos^2\pi\zeta}{1-\cos^2\pi\zeta}\tan\pi\xi ,$$

so that

$$\beta = \frac{\pi}{4}\left[\text{arc tan}\,\frac{1+\cos^2\pi\zeta}{1-\cos^2\pi\zeta}\right]^{-1} . \qquad (15)$$

A comparison of the estimated breadth of reflexions with values of β calculated from this formula is made in Fig. 4. The agreement is satisfactory, considering the difficulty of estimating the breadth of the reflexions and the approximations made in deriving (15). A comparison of calculated and observed intensities, with allowance for instrumental broadening, would require an excessive amount of numerical work. However, it can be shown that for the comparatively sharp reflexions the effect of instrumental broadening will be to make the intensity at the centre of a spot just

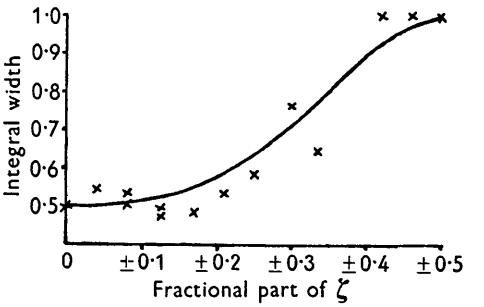

Fig. 4. A comparison of calculated (full line) and observed (crosses) breadths of reflexions.

proportional to $F^2 = (F_R \pm F_L)^2$. A comparison of calculated and observed values of $|F|$ is made in Table 1. The measurements and the calculations for this table were made by Dr M. F. Perutz.

Table 1. *Comparison of calculated and observed values of* $|F|$

$h = 0$	l =	2	4	6	8	10	12	14					
	F_c	24	16	6	10	20	26	12					
	F_o	23	17	6	11	14	28	8					
$h = 10$	l =	0	1	2	3	4	5	6	7	8	9	10	11	12
	F_c	0	9	4	9	16	13	5	1	5	5	4	3	9
	F_o	0	8	5	6	17	16	5	0	6	6	0	0	6
$h = 14$	l =	0	1	2	3	4	5	6	7	8	9			
	F_c	0	19	9	0	4	4	7	2	14	2			
	F_o	0	21	6	0	0	0	5	0	12	0			

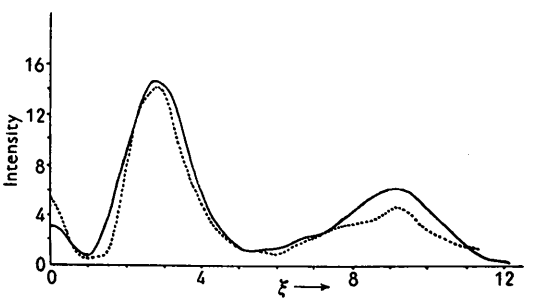

Fig. 5. A comparison of calculated (full line) and observed (dotted line) intensity distributions for the 12th layer line.

The intensity on layer-line 12, for which the factional part of ζ is exactly 0·5, should be given by $F^2 = F_R^2 + F_L^2$. Values of this function for a range of values of ξ are compared in Fig. 5 with the photometrically-measured intensity variation along layer-line 12 of a Buerger precession photograph.

The calculated curve has been corrected for instrumental broadening (the maximum correction was less than 4%). The agreement is seen to be very satisfactory. We consider it unlikely that calculations

based on any other fault-structure for the crystal would agree as well with the observations.

Finally we wish to record our appreciation of the help and advice we have had from Prof. Bragg and Dr Perutz.

References

BRAGG, W. L. & HOWELLS, E. R. (1954). *Acta Cryst.* **7**, 409.

WILSON, A. J. C. (1949). *X-ray Optics*, p. 55. London: Methuen.

Acta Cryst. (1954). **7**, 415

A Note on Deformation Stacking Faults in Hexagonal Close-Packed Lattices

BY J. W. CHRISTIAN

The Inorganic Chemistry Laboratory, Oxford, England

(*Received* 16 *November* 1953 *and in revised form* 20 *January* 1954)

Formulae for the intensity distribution in reciprocal space, and for the integrated intensity and integral breadth of a diffraction maximum, are given for a h.c.-p. structure containing a random distribution of deformation faults.

1. Introduction

The effect of faults in the stacking of the close-packed layers of the f.-c.c and h.c.-p. lattices has been discussed by several authors, especially Wilson (1942, 1949) and Paterson (1952). The diffraction effects depend on the origin of the faults; in particular a distinction has been drawn between 'growth' and 'deformation' faulting (Barrett, 1952). More complex stacking sequences ('extrinsic faults') are also possible (Frank & Nicholas, 1953), but probably have higher energy.

The faulting parameter, α, is defined as the fractional area of all atomic close-packed planes which are faulted. The dissociation of lattice dislocations in close-packed planes gives some faults even in well annealed crystals, but these are insufficient to produce observable diffraction effects. Extensive faulting may be produced by mechanical deformation, martensitic transformation and (possibly) atomic growth. Consideration of the first two of these processes suggests that only deformation faults in both lattices, and h.c.-p. growth faults are likely to be important in practice. Formulae have previously been given for growth faulting in h.c.-p. lattices and for both types of faulting in f.-c.c. lattices. In this note, we give the corresponding formulae for h.c.-p. deformation faulting.

2. Intensity distribution in reciprocal space

We use the same notation as Paterson (1952), except that α is the h.c.-p. faulting parameter, and our vector $\mathbf{a}_3$ is equal to the interplanar translation, so that the factor $\frac{1}{3}h_3$ in his expressions is replaced by h_3. The intensity distribution for $H-K = 3N\pm 1$ may then be written

$$I(HKh_3) = C[J_0 + \sum_1^\infty \{J_m \exp 2\pi i m h_3 + (J_m \exp 2\pi i m h_3)^*\}]$$

and

$$J_m = f^2[P^0_m - \tfrac{1}{2}(P^+_m + P^-_m) \pm i\sqrt{3}.\tfrac{1}{2}.(P^+_m - P^-_m)] .$$

A difference equation for the probabilities P_m may be obtained by considering possible sequences of planes in a manner similar to that used by Paterson. This equation is

$$P^0_m - P^0_{m-2}(1-3\alpha+3\alpha^2) = \alpha-\alpha^2$$

and has solution

$$P^0_m = \tfrac{1}{3} + \frac{2\varrho-1}{6\varrho}\varrho^m + \frac{2\varrho+1}{6\varrho}(-\varrho)^m,$$

where $\varrho = +(1-3\alpha+3\alpha^2)^{\frac{1}{2}}$ and is always real.

Similarly

$$P^+_m = P^-_m = \tfrac{1}{3} + \frac{1-2\varrho}{12\varrho}\varrho^m - \frac{1+2\varrho}{12\varrho}(-\varrho)^m.$$

From this we find

$$J_m = f^2\varrho^m\left[\frac{2\varrho-1}{4\varrho} + (-1)^m\frac{2\varrho+1}{4\varrho}\right],$$

and the intensity distribution in reciprocal space is represented by

$$I(HKh_3) = f^2C\left[1 + \sum_1^\infty \varrho^m\left\{\frac{2\varrho-1}{2\varrho}\cos 2\pi m h_3 + \frac{2\varrho+1}{2\varrho}\cos 2\pi m(h_3+\tfrac{1}{2})\right\}\right]$$

$$= f^2C\left[\frac{(2\varrho-1)(1-\varrho^2)}{4\varrho(1-2\varrho\cos 2\pi h_3+\varrho^2)} + \frac{(2\varrho+1)(1-\varrho^2)}{4\varrho(1-2\varrho\cos 2\pi(h_3+\frac{1}{2})+\varrho^2)}\right]. \quad (1)$$